NISTIR 6417

A Simple Prediction Method For Condensation Heat Transfer Inside A Micro-Fin Tube

F. Marchesi Donati and M.A. Kedzierski

NIST

A Simple Prediction Method For Condensation Heat Transfer Inside A Micro-Fin Tube

F. Marchesi Donati
M. A. Kedzierski

November 1999

Building and Fire Research Laboratory
National Institute of Standards and Technology
Gaithersburg, MD 20899

TABLE OF CONTENTS

ABSTRACT

This study examines an alternative method for modeling in-tube condensation heat transfer. The method's fundamental premise is that the heat flux is directly proportional to the difference between the enthalpy of the vapor at saturated free stream conditions and the enthalpy of the condensed subcooled liquid at the wall. The proportionality coefficient is a pseudo condensation mass velocity. The traditional method for modeling in-tube condensation uses Newton's law of cooling, which defines the heat flux to be directly proportional to the temperature difference rather than the enthalpy difference. Kraay and Rite have used an enthalpy-based expression for the condensation heat flux where the condensation mass velocity was derived from kinetic theory. The present research demonstrates that the kinetic theory approach does not yield realistic results. Consequently, this study presents an alternate energy balance approach is subsequently used to solve for an enthalpy based condensation heat flux. The method reveals that the heat transfer process depends strongly on the derivative of the vapor quality with respect to the distance along the tube axis. Based on this derivation, a correlation is presented that is simpler than those derived from traditional methods. The temperature difference between the free stream vapor and the liquid at the wall does not appear in the correlation.

Keywords: in-tube condensation, kinetic theory, enthalpy-based method, correlation.

NOMENCLATURE

English symbols

A	area (m^2)
c_p	specific heat (J kg^{-1} K^{-1})
D_h	hydraulic diameter (m)
G	mass velocity (kg m^{-2} s^{-1})
i	enthalpy (J kg^{-1})
i_{fg}	latent heat of condensation (J kg^{-1})
h	local single-phase heat-transfer coefficient (W m^{-2} K^{-1})
$h_{2\varphi}$	local two-phase heat-transfer coefficient (W m^{-2} K^{-1})
Ja	refrigerant Jakob number $\dfrac{i_{fg}}{c_p(T_{sat}-T_w)}$ (-)
J_m	mass flux per unit time and per unit area (kg m^{-2} s^{-1})
k	thermal conductivity (W m^{-1} K^{-1})
L	tube length (m)
$\dot{m}$	mass flow rate (kg s^{-1})
M	molecular weight (kg $kmol^{-1}$)
N_f	number of fins (-)
Nu	local Nusselt number based on D_h
P	pressure (Pa) (-)
Pe	Peclet number (Re· Pr)(-)
Pr	liquid refrigerant Prandtl number $\dfrac{c_{p,l}\mu_l}{k_l}$ (-)
p_w	wetted perimeter (m)
q''	local heat flux (W m^{-2})
r	inside radius of the pipe (m)
$r*$	radius of the cylindrical surface equivalent to the actual liquid-vapor interface (m)
R	universal gas constant (N m $mole^{-1}$ K^{-1})
Re	liquid refrigerant Reynolds number $\dfrac{GD_h}{\mu_l}$ (-)
S	perimeter of one fin and channel - measured perpendicular to the fin axis (m)
Sv	non-dimensional refrigerant specific volume $\dfrac{v_g-v_f}{v}$ (-)
St	Stanton number, $\dfrac{h}{\rho Vc_p}$ (-)
T	temperature (K)
$u\infty$	velocity of the vapor at the pipe entrance (m s^{-1})
V	generic velocity (m s^{-1})
x	thermodynamic mass quality (-)
z	axial distance (m)

Greek symbols

Γ	coefficient introduced in Eq. A.4 (-)
δ	turbulent liquid thickness (m)
Δ	λ-δ (m)
λ	thickness of the liquid layer (m)
μ	dynamic viscosity (kg m^{-1} s^{-1})
ν	equilibrium two-phase specific volume $xv_g+(1-x)v_l$ (m^3 kg^{-1})
ρ	density (kg m^{-3})
σ	condensation, or evaporation coefficient introduced in Eq. A.4 (-)

Subscripts

c	condensation
e	evaporation
f	saturated liquid phase
g	saturated vapor phase
glide	due to temperature glide
ig	ideal gas
l	subcooled liquid
lat	latent
r	refrigerant
ref	reference
sat	saturated
sens	sensible
tot	total (liquid and vapor)
w	wall

Introduction

The traditional method to modeling two-phase heat flux was proposed in the early 1700s in an anonymous paper generally attributed to Isaac Newton (Newton, 1701). Newton describes an experiment where the heat transfer between two fluids at different temperatures is observed to be proportional to their temperature difference. Newton's law of cooling is the mathematical expression of this observation. The Newton's law of cooling for a condensation process dictates that the heat flux released by the condensing fluid (q'') can be expressed as the product of the temperature difference between the saturated fluid and the wall (T_{sat}-T_w) and a coefficient of proportionality, which is called heat transfer coefficient, i.e.:

$$q'' = h_{2\varphi}(T_{sat} - T_w) \tag{1}$$

The traditional approach used in studying the two-phase convective heat transfer process consists of predicting the heat transfer coefficient ($h_{2\varphi}$), by correlating it to dimensionless parameters. The two-phase heat transfer coefficient is a function of several parameters, including vapor quality, mass flow-rate, pressure, temperature, and the thermodynamic and transport properties of the fluid. Additionally, the form of the correlation varies with the two-phase flow regimes and the theoretical, semi-theoretical or empirical approach used in modeling the heat transfer. According to Hinde et al. (1992), different forms of correlations can produce predictions that differ by a factor of two or three. A comprehensive review of the state of the art is presented in Dobson and Chato (1998). The drawback to the traditional approach is that the heat transfer coefficient correlation is affected by (1) the choice of the dimensionless parameters for its functional form and (2) the choice of the approach to be used. It is clear that the considerable difference between prediction methods causes uncertainty in the rating and sizing of heat exchangers. As a result, condensers are usually oversized to meet the required duty.

To overcome the disadvantages of the traditional approach to correlating the two-phase heat transfer process, Kraay and Rite (1997) proposed a new methodology in which the heat flux is assumed to be proportional to the difference between the enthalpy of the vapor at free stream conditions and the enthalpy of the condensed liquid at the wall:

$$q'' = J_m \Delta i \tag{2}$$

The coefficient of proportionality, J_m, represents the flux of mass per unit time or mass velocity from a point at the free stream conditions to a point at wall conditions. The advantage of the Kraay and Ray method for modeling condensation is that it accounts separately for the phase change heat transfer and the liquid subcooling heat transfer. The traditional temperature based heat transfer equation cannot be used to describe the phase change alone because the phase change occurs at essentially no temperature difference.

Kraay and Rite (1997) claim that their approach allows the parameter that they refer to as a "new heat transfer coefficient," J_m, to depend only on flow rate, fluid properties, and wall geometry, rather that being a function of local vapor quality. They studied the latent heat transfer at the interface by using the kinetic theory of condensation (this approach is described in the Appendices). It is difficult to rigorously apply the kinetic theory to convective condensation. For example, the kinetic theory of condensation is well developed for the cases in which the velocity of the condensing vapor has no component tangent to the liquid-vapor interface and where the condensation process is independent of vapor quality. Unfortunately, in-tube condensation is a strong function of vapor quality and exhibits significant tangential vapor velocities. To compensate for this, Kraay and Rite (1997) revert to several assumptions to adapt the kinetic theory to in-tube condensation, which are not always easy to justify.

The current study has two objectives. The first objective is to review the proposed kinetic theory based model for in-tube condensation. The second objective is to develop an energy-based model for in-tube condensation. The focus of the energy-based model is the determination of an expression for the mass velocity J_m.

Derivation Of An Alternative Heat Transfer Equation For Pure Fluids And Near Azeotropes

In deriving a practical and usable expression for J_m, the Kraay and Rite (1997) theory contains several unrealistic assumptions. Consequently, this paper proposes an alternative method for calculating J_m. The new method retains the basic approach that has been outlined by Kraay and Rite's (1997): the total heat flux is a sum of the single phase subcooling and the two-phase

condensation. Both the sensible and latent heat fluxes are based on an enthalpy difference, rather than a temperature as the driving potential for heat transfer. The method proposed in this study differs from Kraay and Rite's (1997) because the coefficient J_m's expression is derived from mass and heat balances rather than from the kinetic theory.

As stated above, the total heat that a condensing fluid exchanges with the cooling fluid can be separated into the latent and the sensible heats:

$$q'' = J_{m_{lat}} \cdot i_{fg} \tag{3}$$

and

$$q'' = J_{m_{sens}} \cdot (i_f - i_{fw}) \tag{4}$$

The potential for the latent heat transfer is the enthalpy difference between the vapor and the liquid, while the potential for the subcooling energy transfer is the enthalpy difference between saturated liquid and subcooled liquid (wall conditions). The corresponding $J_{m_{lat}}$ and $J_{m_{sens}}$ are functions of the distance along the pipe (z), because these coefficients vary with the vapor quality.

The expression for $J_{m_{lat}}$ can be found by a simple mass balance. Figure 1 represents an element of liquid of length dz, which lies along the tube wall. Liquid enters the element from the left side and flows along the wall. Condensed vapor ($\dot{m}_L|_z$) enters the top to the element and is equivalent to $J_{m_{lat}}$ multiplied by the area of the liquid-vapor interface (dA). Liquid exits the right side of the element at a location $z+dz$, (i.e., $\dot{m}_L|_{z+dz}$).

The mass that goes from vapor to liquid per unit time and per unit area ($J_{m_{lat}}$), can then be written in terms of the variation of the liquid mass flux $\dot{m}_L|_z$ along the pipe as:

$$J_{m_{lat}}|_z \cdot dA|_z = d\dot{m}_L|_z \tag{5}$$

Regardless of the flow pattern of the fluid inside the pipe, the area of the interface between liquid and vapor can be written as $2\pi r^* dz$.

$$J_{m_{lat}} \cdot 2 \cdot \pi \cdot r^* \cdot dz = d\dot{m}_L \tag{6}$$

7

$$J_{m_{lat}} = \frac{dm_L}{2 \cdot \pi \cdot r^* \cdot dz} \tag{7}$$

The relationship between the vapor quality x and the liquid mass flux is:

$$\frac{dx}{dz} = -\frac{1}{m_{tot}} \frac{dm_L}{dz} \tag{8}$$

Substitution of Eq. 6 into Eq. 8 gives an expression for $J_{m_{lat}}$:

$$J_{m_{lat}} = -\frac{m_{tot}}{2 \cdot \pi \cdot r^*} \frac{dx}{dz} \tag{9}$$

The relationship between the latent heat transfer coefficient and the sensible heat transfer coefficient is found by means of an energy balance. Consider the control volume shown in Fig. 2. The enthalpy of the bulk fluid is assumed to be a linear combination of the wall and saturated liquid enthalpy, as shown in Eq. 10:

$$i|_z = i_f|_z \, k + i_{fw}|_z \, (1-k) \tag{10}$$

The coefficient k can have any value between 0 and 1, while $i_{fw}(z)$ is evaluated at the wall temperature and at a pressure which is 90 % of the pressure of the vapor phase. This last assumption is validated by the fact that the ratio of the pressure of the liquid just under the vapor-liquid interface to that of the gas is about 0.9 for a low velocity of the vapor toward the interface (Ytrehus and Østmo, 1996) as predicted by the kinetic theory of condensation.

The heat balance from Fig. 2 has the expression:

$$dq_{lat} + \dot{m}_L|_z \cdot i|_z + d\dot{m}_L|_z \cdot i_f|_z = \dot{m}_L|_{z+dz} \cdot i|_{z+dz} + dq_{tot} \tag{11}$$

Because $dq_{tot} = dq_{lat} + dq_{sens}$, Eq. 11 can be simplified as:

$$dq_{sens} = -\frac{d[\dot{m}_L|_z \cdot i|_z]}{dz} dz + d\dot{m}_L|_z \cdot i|_z \tag{12}$$

Dividing by dz and expanding the derivative of the first term on the right side, Eq. 12 becomes:

$$\frac{dq_{sens}}{dz} = -\frac{d[\dot{m}_L|_z]}{dz} i|_z - \frac{d[i|_z]}{dz} \dot{m}_L|_z + \frac{d\dot{m}_L|_z}{dz}|_z \cdot i_f|_z \tag{13}$$

Dividing each term of Eq. 13 by the circumference of the vapor-liquid interface, the left side of Eq. 13 represents the sensible heat flux through the liquid-vapor interface area.

$$\frac{dq_{sens}}{dz}\frac{1}{2\pi r*} = \frac{1}{2\pi r*}\frac{d[m_L|_z]}{dz}(i_f|_z - i|_z) - \frac{1}{2\pi r*}\frac{d[i|_z]}{dz}m_L|_z \tag{14}$$

Since $J_{m_{sens}}$ is defined as:

$$J_{m_{sens}} = \frac{q''_{sens}}{i_f|_z - i_{fw}|_z} \tag{15}$$

Eq. 14 is equivalent to the following expression for the sensible heat molecular flux:

$$J_{m_{sens}} = \frac{1}{2\pi r*}\frac{d[m_L|_z]}{dz}\left(\frac{i_f|_z - i|_z}{i_f|_z - i_{fw}|_z}\right) - \frac{m_L|_z}{2\pi r*}\frac{d[i|_z]}{dz}\frac{1}{i_f|_z - i_{fw}|_z} \tag{16}$$

To correctly sum the sensible and latent heat ($q''2\pi rdz$), they must refer to the same area, i.e., the area of the liquid-vapor interface ($2\pi r*dz$).

$$q''\frac{2\pi r \cdot dz}{2\pi r* \cdot dz} = q''\frac{r}{r*} \tag{17}$$

The heat flux balance is then:

$$q''\frac{r}{r*} = J_{m_{tot}}i_{fg} + \frac{1}{2\pi r*}\frac{d[\dot{m}_L|_z]}{dz}(i_f|_z - i|_z) - \frac{1}{2\pi r*}\frac{d[i|_z]}{dz}\dot{m}_L|_z \tag{18}$$

Substituting Eq. 9 into Eq. 18, and remembering that $m_L|_z = m_{tot}\cdot(1 - x|_z)$ gives:

$$q''\frac{r}{r*} = -\frac{\dot{m}_{tot}}{2\pi r*}\frac{dx}{dz}(i_g|_z - i_f|_z) - \frac{m_{tot}}{2\pi r*}\frac{d[m_{tot}]}{dz}\frac{dx}{dz}(i_f|_z - i|_z) - \frac{m_{tot}}{2\pi r*}\frac{d[i|_z]}{dz}(1 - x) \tag{19}$$

Simplifying Eq. 19 gives:

$$q'' = -\frac{\dot{m}_{tot}}{2\pi r}\left\{\frac{dx}{dz}(i_g|_z - i|_z) + \frac{d[i|_z]}{dz}(1 - x)\right\} \tag{20}$$

Equation 20 represents the heat balance equation for the condensing fluid.

The data presented by Kedzierski and Gonclaves (1999) were used to validate the model given by Eq. 20. These data are from counterflow tests of R32 flowing in a micro-fin tube. The local heat transfer coefficient was measured at twelve x-positions along the tube for each run. Figure 3 compares the experimental heat flux versus the length of the pipe to that calculated from Eq. 20. The value of k chosen for this comparison is 0.9. The agreement between the measured heat flux and the model chosen for the heat balance is within 2 %. The calculations show that the choice for the value of k in Eq. 20 does not greatly influence the results (q'' is an implicit function of k,

because the bulk enthalpy $i|_z$ is a function of k). This is due to the fact that the percentage of the sensible heat transfer exchanged over the total (from 2 % to 7 %) is small compared to the latent. Therefore, in the following derivation, the value of k will be set to 0.9.

The same model has been verified for other refrigerants, including R134a, and for a parallel flow configuration as well. For all the tested refrigerants and configurations, the agreement between the model and the experimental data was within 2 %.

Equation 20 has also been validated for zeotropic refrigerant mixtures with small temperature glides i.e., near-azeotropic mixtures such as R410A. The sensible heat due to the change in composition of the vapor has to be added for mixtures with significant temperature glides, e.g., R407C. For this reason, the derivation of the heat balance equation for the zeotropic refrigerant mixtures is dealt with in the following section.

Derivation Of An Alternative Heat Transfer Equation For Zeotropic Mixtures

During condensation, the total heat released by a zeotropic mixture to the cooling fluid is the sum of: (1) the latent heat, (2) the sensible heat in the liquid, and (3) the sensible heat due to the temperature glide. Once the variation in composition as a function of the vapor quality along the pipe is known, the enthalpy of the liquid can be written as function of the vapor quality and inserted in the heat flux balances equation.

Equation 14 can be rewritten for zeotropic mixtures as:

$$\frac{1}{2\pi r^*}\frac{d\left[\dot{m}_L|_z\right]}{dz}(i_f(x|_z)-i(x|_z))-\frac{1}{2\pi r^*}\frac{d[i(x|_z)]}{dz}\dot{m}_L(z)=\frac{dq_{sens}}{dz}\frac{1}{2\pi r^*} \tag{21}$$

After applying the chain rule to the derivative on the second term on the left side of the Eq. 21, the final expression for the sensible heat transferred in the liquid, due to either subcooling or to the composition change (i.e., due to the glide in the liquid) is:

$$\frac{1}{2\pi r^*}\frac{d\left[m_L|_z\right]}{dz}(i_f(x|_z)-i(x|_z))-\frac{1}{2\pi r^*}\frac{d[i(x|_z)]}{dx}\frac{dx}{dz}m_L|_z=\frac{dq_{sens}}{dz}\frac{1}{2\pi r^*} \tag{22}$$

To find an expression for the heat due to the glide, a vapor element of length dz is to be considered, with the interface included in the element.

For a fixed overall mixture composition, performing a heat balance on the vapor element gives:

$$m_v|_z \cdot i_g(x|_z) = m_v|_{z+dz} \cdot i_g(x|_{z+dz}) + dq_{lat} + dm_v i_f(x|_z) + dq_{glide} \tag{23}$$

where the sensible heat due to the glide is expressed as dq_{glide}.

Substituting the expression for dq_{lat} (Eq. 9) into Eq. 23 and rearranging gives:

$$\frac{dq_{glide}}{dz} = -m_v \frac{di_g(x|_z)}{dx} \frac{dx}{dz} \tag{24}$$

Since $m_v|_z = m_{tot} \cdot x|_z$, the derivative of the glide heat along the pipe is:

$$\frac{dq_{glide}}{dz} = -m_{tot} x|_z \frac{di_g(x|_z)}{dx} \frac{dx}{dz} \tag{25}$$

For zeotropic mixtures, the heat balance equation is:

$$dq''_{tot} = dq''_{lat} + dq''_{sens} + dq''_{glide} \tag{26}$$

Substituting into Eq. 26 the expressions for dq''_{lat} and dq''_{sens} and the above term gives:

$$q'' \frac{r}{r*} = -\frac{\dot{m}_{tot}}{2\pi r*} \frac{dx}{dz}(i_g(x|_z) - i_f(x|_z)) - \frac{\dot{m}_{tot}}{2\pi r*} \frac{dx}{dz}(i_f(x|_z) - i(x|_z) -$$

$$-\frac{\dot{m}}{2\pi r*}(1-x)\frac{di(x|_z)}{dx}\frac{dx}{dz} - \frac{\dot{m}}{2\pi r*}x\frac{di_g(x|_z)}{dx}\frac{dx}{dz} \tag{27}$$

Combining the common terms, an implicit differential equation for x that applies to zeotropic mixtures is:

$$-\frac{\dot{m}_{tot}}{2\pi r}\frac{dx}{dz}\left[(i(x|_z) - i_g(x|_z)) + x \cdot \left(\frac{di(x|_z)}{dx} + \frac{di_g(x|_z)}{dx} \right) \right] = q'' \tag{28}$$

Description Of The Experimental Apparatus Used To Validate The Enthalpy-Based Heat Transfer Model

In this section, the enthalpy based energy balances for pure fluids and near azeotropes provides the basis for correlation of the local tube-side condensation data of Kedzierski and Gonclaves (1999). These data were obtained with an experimental apparatus used to establish and measure the convective condensation for R134a and the near-azeotropic refrigerant mixture R410A, along with its pure components R32 and R125.

The Kedzierski and Gonclaves (1999) test section consisted of a pair of 3.34 m long, horizontal tubes connected by a U-bend. A magnetically coupled gear pump delivered the test refrigerant to the entrance of the test section with a few degrees of vapor superheat. Another magnetically coupled gear pump supplied a steady flow of water to the test section. The inlet temperature of the water loop was held constant for each test with a water-chilled heat exchanger and variable electric heaters. The refrigerant and the water flow rates were controlled with continuously variable speed pumps. Redundant flow rate measurements were made with Coriolis and turbine flow meters on both the refrigerant and the water- sides.

The test refrigerant flowed inside a micro-fin tube, while water flowed either in counterflow or in parallel flow to the refrigerant in the annulus that surrounds the micro-fin tube. The annulus gap was 2.2 mm, and the micro-fin tube wall thickness was 0.3 mm. The micro-fin tube had 60, 0.2 mm high fins. For such a geometry, the cross sectional area is 60.8 mm^2 giving an equivalent smooth diameter of 8.8 mm and a wetted perimeter of 44.23 mm. The root diameter of the micro-fin tube was 8.9 mm. The inside surface area per unit length of the tube was estimated to be 5.23 mm. The ratio of the wetted perimenter of the micro-fin tube to that of a smooth tube with an equivalent hydraulic diameter was 1.6. The fins rifled down the axis of the tube at a helix angle of 18° with respect to the tube axis.

Heat Transfer Correlation

Over 1000 data points from the above-described experimental study were used to develop a heat transfer correlation that is based on the model expressed by Eq. 20. The variable to be correlated is the derivative of the vapor quality with respect to the length of the pipe, $\frac{dx}{dz}$. The quality derivative represents the mass of the vapor condensed per unit of length. The values of $\frac{dx}{dz}$ to be correlated, according to Eq. 35, were calculated from the experimental data of Kedzierski and Gonclaves (1999). All the heat exchanged has been considered to be latent. Such a choice is mainly based on the observation that the sensible term is a small percentage of the total heat exchanged. From the analysis of the data, it was noted that for the pure fluids R32, R134a, and

R125, the sensible heat flux corresponds in average to the 3 % of the total heat exchanged in the experimental quality range (0.05-0.99). For mixtures, the fraction of sensible heat increases to 6 %. Even if neglecting the sensible heat introduces a systematic error in estimating $\frac{dx}{dz}$, the derivation of such a quantity from the actual derivative of the vapor quality introduces considerable and unpredictable uncertainty for very low and very high vapor quality values, i.e. at the extremes of the function to be derived.

The actual quantity which is correlated is $\frac{dx}{dz} \cdot Ja \cdot D_h$. The presence of D_h in the quantity to be correlated allows $\frac{dx}{dz} \cdot Ja \cdot D_h$ to be nondimensional. The Jakob number is present in the quantity to be correlated, through preliminary analysis of $\frac{dx}{dz} D_h$ revealed a variation it was found that the exponent on Ja that was nearly Ja^{-1}.

The first pass for the search of the form of the correlation is done using only those data points with an estimated expanded uncertainty for the traditional Nu that are less than 25%. Next, the 686 omitted measurements are predicted with the same regression using dimensionless parameters. Those excluded measurements that are predicted to within ±25% of the first correlation are reintroduced into the regression data set. New coefficients are then generated using 1317 measurements of the regression data set. The hat matrix and the Cook's distance are generated for the second regression and used to determine the data that has have high-leverage and influence on the model, respectively. The diagonal elements of the hat matrix that are greater than approximately $\frac{2d}{n}$, where d is the number of model parameters and n is the number of data points, are designated as high leverage points (Belsey et al., 1982). The elements of the Cook's array that are greater than $\frac{4}{n}$ are considered to be influential observations. A total of 1218 points are left for the final form of the correlation.

The form of the correlation was obtained by following the approach of Cooper (1984). Cooper (1984) suggests that the fluid properties that govern nucleate pool boiling can be well represented by a product of the acentric factor and other dimensionless variable to various powers. The present correlation has the form:

$$\frac{dx}{dz} \cdot D_h \cdot Ja = \alpha_1 \cdot Re_l^{\alpha_2} \cdot Pr^{\alpha_3} \cdot Sv^{\alpha_4} \cdot \left(-Log_{10}\left(\frac{p_r}{p_c}\right) \right)^{\alpha_5} \tag{29}$$

where:

$$\alpha_1 = 5.1081$$
$$\alpha_2 = -0.783242$$
$$\alpha_3 = -0.708893$$
$$\alpha_4 = -0.606725$$
$$\alpha_5 = 0.461457$$

The expanded uncertainty of the fit for 95 % confidence is approximately ± 21 %.

Figure 5 compares the experimental $\frac{dx}{dz}$ to the predicted values (Eq. 29). The expanded

uncertainty of $\frac{dx}{dz}$ for 95 % confidence was approximately ± 8 %. For high values of the quantity

$\frac{dx}{dz}$ the correlation predicts a different behavior for counterflow and parallel flow data, which was

also the case in the work presented by Kedzierski and Gonclaves (1999). The difference is appreciable in the low vapor quality regions for counterflow conditions and in the high quality region for parallel flow conditions, as shown in Fig. 6, which represents the trend of the derivative of the vapor quality versus the vapor quality itself.

Figure 7 compares the measured condensation Nusselt number with the Nusselt number predicted by Eq. 29. The expanded uncertainty of the measured Nu for 95% confidence was approximately 16%. Only random trends are observed in the residuals plots against each of the parameters of Eq. 29.

The present correlation was compared to the data that were used to generate it. Figure 8 compares the heat transfer coefficient versus quality for the four test fluids at $G_r = 250$ kg/m^{2}s and $T_r = 40$ °C. The lines are predictions for the present micro-fin tube geometry which were

obtained form the correlation of the data given as Eq. 29. In general, the Nusselt number decreases for decreasing qualities because the liquid layer becomes thicker as the quality decreases. A greater heat transfer resistance occurs for the thicker condensate films. Furthermore, R32 exhibits the higher heat transfer coefficient, due to its high thermal conductivity and low liquid viscosity. The R125 has the poorest heat transfer, while the mixture R410A (R32/R125, 50/50 composition by mass) has a performance which lies in between those of its pure components. These trends are consistent with those reported by Kedzierski and Gonclaves (1999).

From their relationship to the traditional heat transfer coefficient, the relation between the Nusselt number and $\dfrac{dx}{dz}$ is expressed by Eq. 30:

$$\frac{dx}{dz} = Nu \cdot \frac{p_w \cdot k_l}{m \cdot c_p} \cdot \frac{1}{D_h J_a}$$ (30)

Substituting Eq. 30 into Eq. 29, an expression for the Nusselt number can be derived as:

$$Nu = \frac{D_h}{D_h} \cdot \frac{mc_p}{p_w k_l} \cdot \alpha_1 \cdot Re_l^{\alpha_2} \cdot Pr^{\alpha_3} \cdot Sv^{\alpha_4} \cdot \left(-Log_{10}\left(\frac{p_r}{p_c} \right) \right)^{\alpha_5}$$ (31)

The hydraulic diameter cancels out, and the term $\dfrac{mc_p}{p_w k_l}$ be related to the Peclet number (see Kedzierski and Gonclaves (1999)):

$$\frac{mc_p}{p_w k_l} = Re \cdot Pr \cdot \frac{N_f \cdot S}{4\cos\alpha \cdot p_w} = Pe \cdot \frac{N_f \cdot S}{4\cos\alpha \cdot p_w} = \frac{Pe}{4}$$ (32)

Substituting Eq. 32 into Eq. 30 the final expression for the Nu number is:

$$Nu = \frac{1}{4} \cdot \alpha_1 \cdot Re_l^{\alpha_2^{*}} \cdot Pr^{\alpha_3^{*}} \cdot Sv^{\alpha_4} \cdot \left(-Log_{10}\left(\frac{p_r}{p_c} \right) \right)^{\alpha_5}$$ (33)

where the new exponents for the Reynolds and the Prandtl numbers are:

$$\alpha_2^{*} = -0.783242 + 1 = 0.216758$$
$$\alpha_3^{*} = -0.708893 + 1 = 0.291107$$

Figure 9 represents a comparison of the correlation expressed by Eq. 33 with data from Eckels and Tesene (1998). The systematic underprediction of the Eckels and Tesene (1998) data by Eq. 33 could be due to experimental differences between the data that was used to generate Eq. 33 and the Eckels and Tesene (1998) data. Baker's (1954) flow map and Soliman's (1982, 1983 & 1986) flow transition correlations for smooth tubes are used to approximately determine the flow conditions. Baker's results showed that 79 %, 18 %, 2 %, 1 % of the data are respectively in annular, slug, bubbly and wavy flow conditions. Soliman's correlations indicated that 47 %, 30 %, and 23 % of the data are in wavy (stratified, slug, wavy), annular, and mist flow conditions, respectively. No reduction in the residual standard deviation of the *Nu* regression is obtained when the data set is reduced to only the annular flow (as indicated by the Soliman correlations) data.

The correlation which has been presented in Eq. 33 is now compared with the one proposed by Cavallini et al. (1997). These authors correlate the Nusselt number with 5 variables, Re_{eq}, Pr_l, Rx, Bo, Fr. These are, respectively, the equivalent Reynolds number, the liquid Prandtl number, a geometrical parameter, the Bond Number and the Froude number. For an accurate description of the parameters used, refer to Cavallini et al. (1997). The correlation for the Nusselt number is:

$$Nu = 0.05 \cdot \text{Re}_{eq}^{0.8} \, \text{Pr}^{1/3} \, Rx^2 (Bo \cdot Fr)^{-0.26} \tag{34}$$

Figure 10 shows that if the above expression for the *Nu* number, given by Cavallini et al. (1997), is used in Eq. 30, the $\dfrac{dx}{dz}$ values are overpredicted by approximately 200 % to 400 %.

Conclusions

An alternative correlation method for the in-tube condensation heat transfer coefficient which offers some advantages over the traditional method has been presented. The alternative approach correlates a physical quantity, $\frac{dx}{dz}$, rather a mathematical definition as is done in the traditional Newton's law of cooling approach. The correlation that results from the alternative method is much simpler than one that is obtained from correlating the Nusselt number directly. For example, the vapor quality does not appear in the exponents of the non-dimensional parameters selected for the correlation, while in the traditional method, the presence of the vapor quality in the exponents is essential. Another improvement with respect to the traditional approach is that the Jakob number does not appear in the correlation. The benefit that is realized from this is that an iterative procedure is not necessary to calculate the temperature difference between the saturated vapor and the tube wall.

References

O. Baker, Simultaneous flow of oil and gas, The oil and gas journal, Vol. 53, p. 85, 1954

D. A. Belsey, E. Kuth, R. E. Welsch, Regression diagnostics: Identifying Influential Data and Sources of Collinearity, New York, Wiley, 1980.

D. Butterworth, G. F. Hewitt Editors, Two phase flow and heat transfer, Oxford University Press, 1977.

A. Cavallini, D. Del Col, L. Doretti, G. A. Longo, L. Rossetto, A new model for refrigerant condensation inside enhanced tubes, Proceedings XV UIT National Heat Transfer Conference, Vol. 1, p. 521, 1997.

J. G. Collier, J. R. Thome, Convective boiling and condensation, Third Edition, Clarendon Publication, Oxford, 1992.

M. G. Cooper, Saturation nucleate pool boiling, a simple correlation, Vol. 86, Department of Engineering Science, Oxford University, England, p. 785.

M. K. Dobson, J. C. Chato, Condensation on smoothes horizontal tubes, J. Heat Transfer, Vol. 120, n. 1, pp.193-213, 1998.

S. J. Eckels, B. Tesene, Q. Wang, In-tube condensation of refrigerants in smooth and enhanced tubes, ASHRAE New Investigator Report, July 1998.

H. Hertz, Ueber die Verdunstung der Flüssigkeiten, insbesondere des Quecksilbers, Annales Phys. Chem., Vol. 17, p. 177, 1882.

D. K. Hinde, M. K. Dobson, J. C. Chato, M. E. Mainland, Rhines N., Condensation of R-134a with and without oils, ACRC Technical Report 26, University of Illinois at Urbana-Champain, 1992.

M. A. Kedzierki, J. M. Gonclaves, Horizontal convective condensation of alternative refrigerant mixtures within a micro-film tube, Journal of Enhanced heat transfer, Vol. 6, No. 2-4, pp 161-178, 1999.

M. Knudsen, Die Maximale Verdampfungsgeschwindigkeit des Quecksilbers, Annales Phys, Chem., Vol. 47, p. 697, 1915.

M. L. Kraay, R. W. Rite, Personal communication, June 1997.

I. Newton, 1701, " Scala Graduum Caloris", The Philosophical Transaction of the Royal Society of London, Vol. 22, pp. 824-829, Translated from latin in The Philosophical Transaction of the Royal Society of London, Abridged, Vol. IV (1694-1702), London, 1809, p. 572.

R.W. Schrage, A theoretical study of interphase mass transfer, Columbia University Press, New York, 1953.

H. M. Soliman, On the annular-to-wavy flow pattern transition during condensation inside horizontal tubes, The Canadian Journal of Chemical Engineering, Vol. 60, p. 457, 1982.

H. M. Soliman, Correlation of Mist-Annular Transition during Condensation, The Canadian Journal of Chemical Engineering, Vol. 61, p. 178, 1983.

H. M. Soliman, The Mist-Annular Transition During Condensation, and its influence on the Heat transfer Mechanism, International Journal of Multi-phase flow Vol. 12, n. 2, p. 277, 1986.

D. J. Wilhelm, Condensation of metal vapors and kinetic theory of condensation, Argonne National Laboratory report #6948

T. Ytrehus, S. Østmo, Kinetic theory approach to interphase processes, International Journal of Multiphase Flow, Vol. 22, n. 1, p. 133, 1996.

Acknowledgments

$$J_{m,lat}\, \mathrm{d}A$$

$\mathrm{d}m_L(z)$ → → $\mathrm{d}m_L(z + \mathrm{d}z)$

$\mathrm{d}z$

Figure 1-Mass balance on a differential liquid element

$dq_{lat}|_z$ $d\dot{m}_L|_z\, i_f|_z$
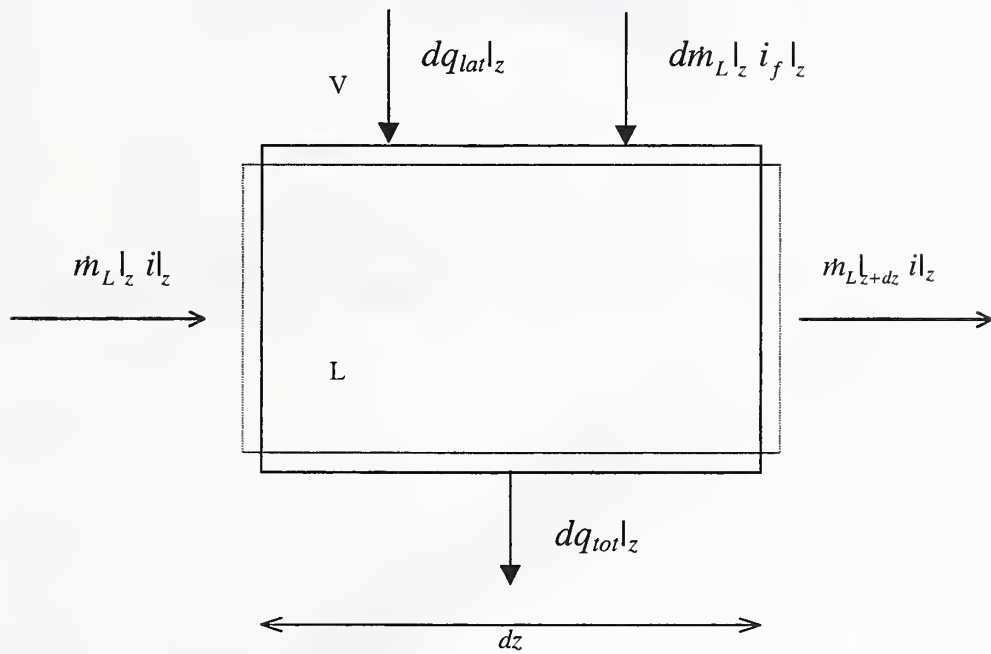
V

$\dot{m}_L|_z\, i|_z$ L $\dot{m}_L|_{z+dz}\, i|_z$

$dq_{tot}|_z$

dz

Figure 2- Heat balance on a liquid element
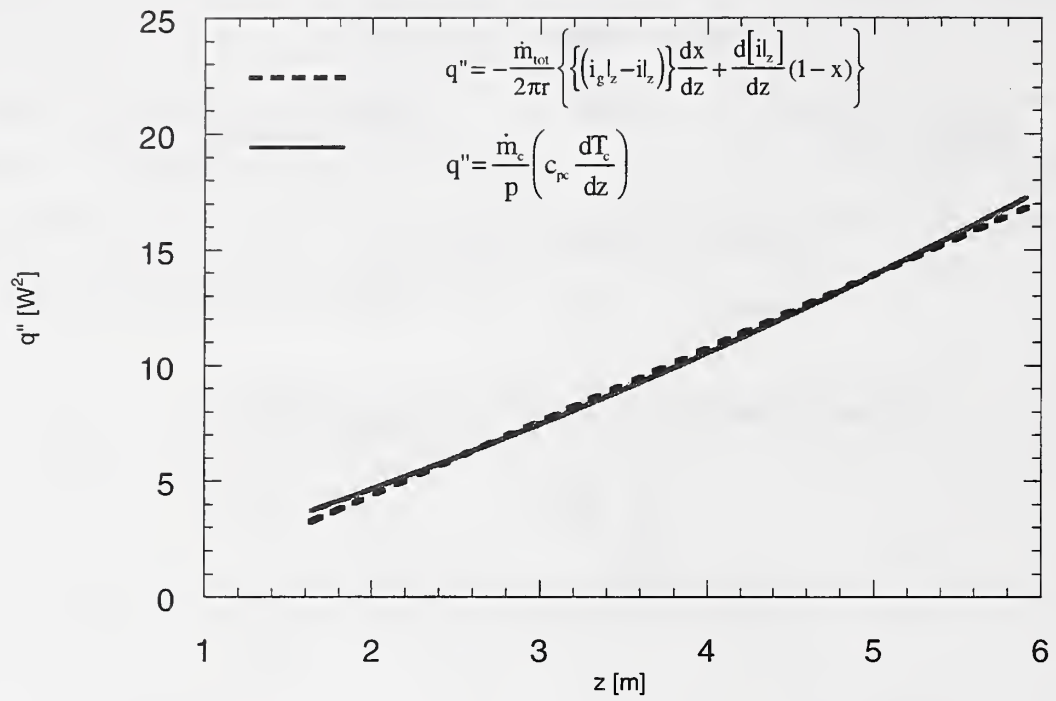
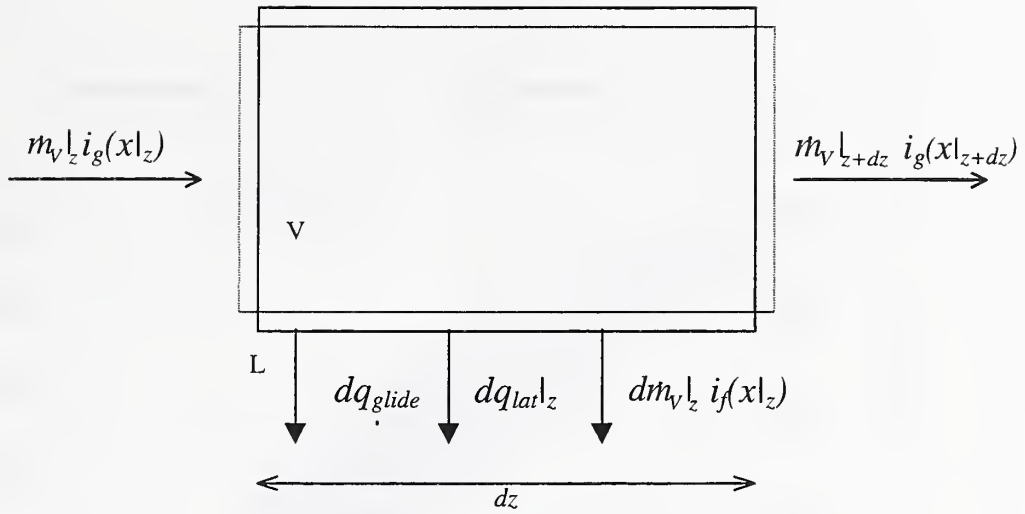Figure 3- Heat flux based on a heat transfer fluid calometric and Eq. (20)

$$m_V|_z \, i_g(x|_z) \longrightarrow \qquad m_V|_{z+dz} \, i_g(x|_{z+dz})$$

V

L

$$dq_{glide} \qquad dq_{lat}|_z \qquad dm_V|_z \, i_f(x|_z)$$

$$dz$$

Figure 4- Heat balance on a vapor element
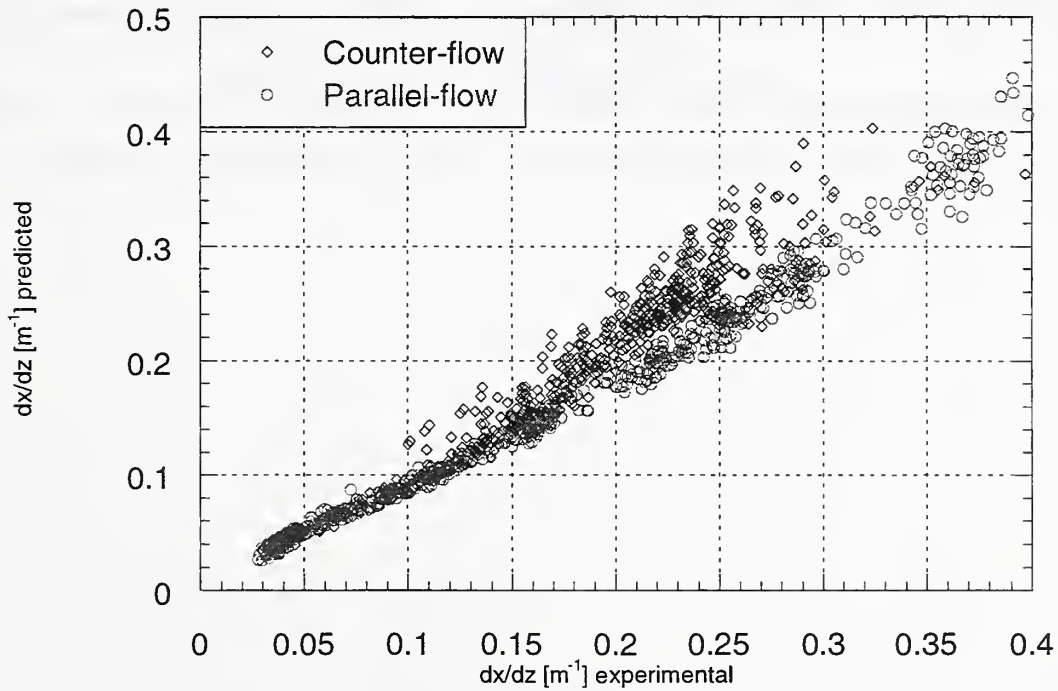
Figure 5- Comparison of measured and predicted $\dfrac{dx}{dz}$, Micro-fin tube, R32, R125, R134a, R410A
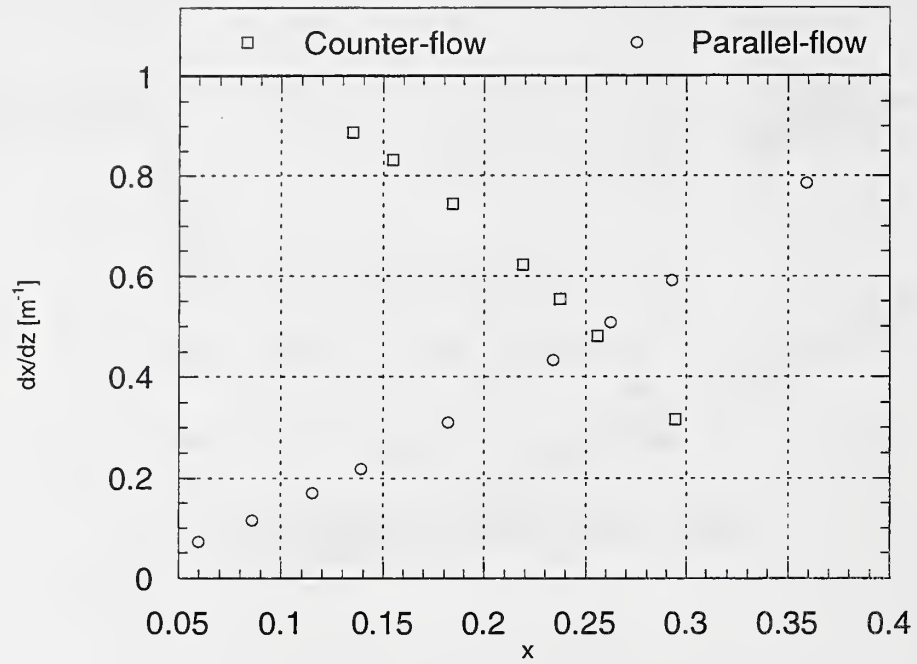
condensation, $\alpha=18°$, $D_h=5.45$, Re=7715

Figure 6- $\dfrac{dx}{dz}$ vs vapor quality for parallel flow and counterflow. Counterflow Re=9100,
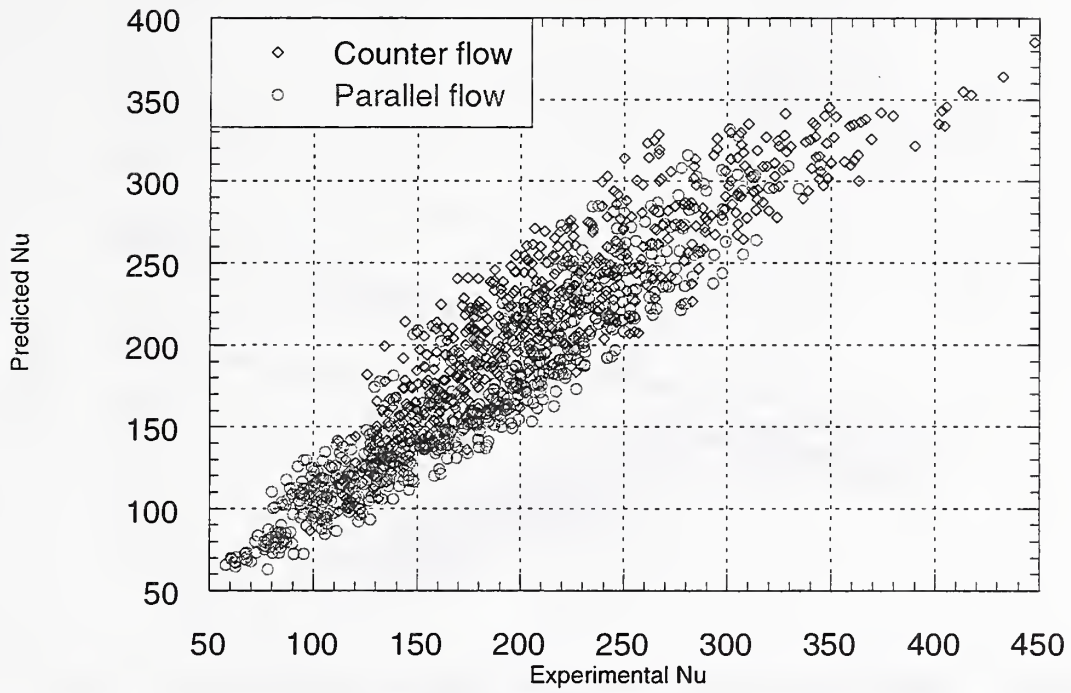
Pr=0.427; Parallel flow Re=13230, Pr=0.561

Figure 7-Comparison of measured and predicted convective condensation Nusselt numbers.
Micro-fin tube, R32, R125, R134a, R410A condensation, $\alpha=18°$, $D_h=5.45$, Re=7715
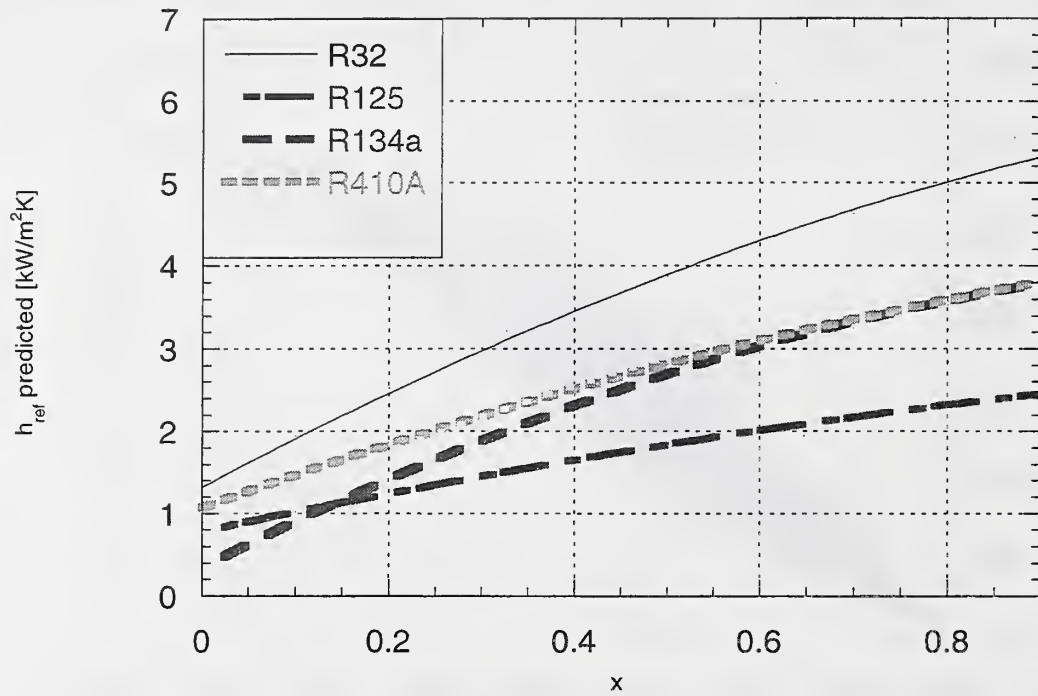
Figure 8- Comparison of the heat-transfer coefficient h_{ref} for different fluids versus thermodynamic quality
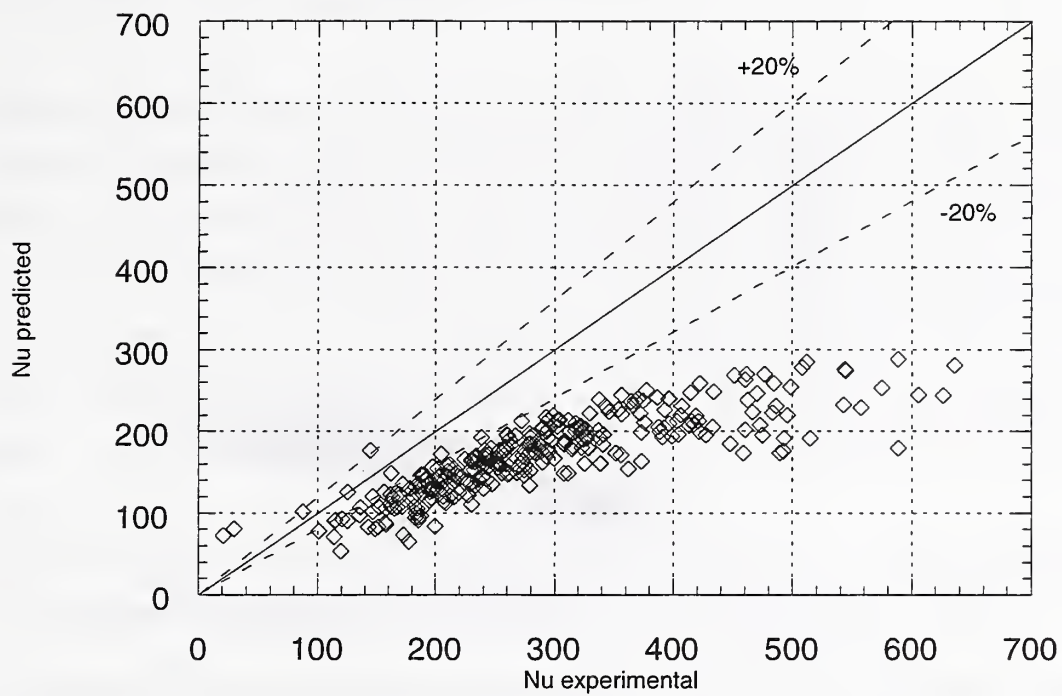
Figure 9- Comparison experimental Nusselt numbers and the predictions of Eq. (33).
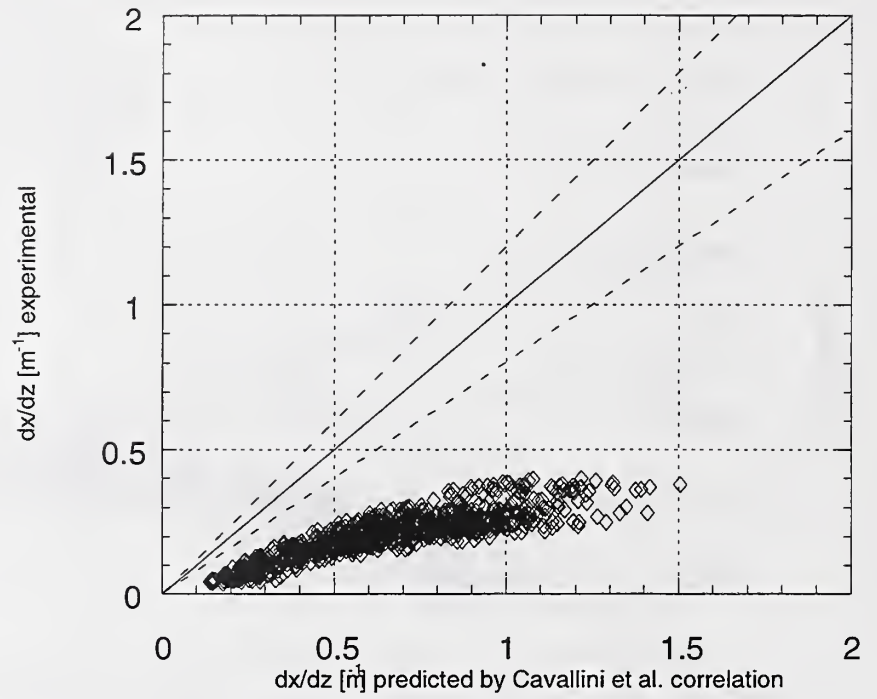
Fig. 10- Comparison of experimental Kedzierski and Gonclaves (1999) $\dfrac{dx}{dz}$ data with the predictions of Eq. (34) (Cavallini, 1997).

Appendix A: Review Of The Kinetic Theory Of Condensation

The kinetic theory of condensation is reported in several publications (Collier and Thome, 1992, and Wilhelm, 1962). To be complete, a brief review of the principal concepts of the kinetic theory of condensation is reported below.

Consider a pure saturated vapor with pressure P_g and temperature T_g in equilibrium with its own liquid phase. The liquid temperature at the liquid-vapor interface is T_f. Due to thermodynamic equilibrium, the liquid moles that cross the liquid-vapor interface into the vapor space are balanced by an equal number of moles that move from the vapor into the liquid. Condensation occurs if the flux of molecules from the vapor to the liquid phase (J_{m+}) exceeds the flux of the molecules from the liquid to the vapor phase (J_{m-}). Figure A.1 illustrates the condensation process. The net or the condensation molecular flux across the vapor-liquid interface is:

$$J_m = J_{m+} - J_{m-} \tag{A.1}$$

Using the kinetic theory of condensation, Hertz (1882)-Knudsen (1915) demonstrated that the molecular flow rate of a stagnant perfect gas through an imaginary plane is given by:

$$\left| J_m \right| = \left(\frac{M}{2\pi R} \right)^{1/2} \frac{P}{T^{1/2}} \tag{A.2}$$

where $\left| J_m \right|$ is the flux of mass in either direction perpendicular to the plane, M is the molecular weight; R is the universal gas constant; and P and T are the absolute pressure and the absolute temperature, respectively.

Substitution of the Hertz-Knudsen equation (Eq. A.2) into the mass flux balance (Eq. A.1), where J_{m+} is the flux from vapor to liquid and J_{m-} is the flux from liquid to vapor, gives:

$$J_m = \left(\frac{M}{2\pi R} \right)^{1/2} \left[\frac{P_g}{T_g^{1/2}} - \frac{P_f}{T_f^{1/2}} \right] \tag{A.3}$$

Schrage (1953) modified the Hertz-Knudsen equation to account for the effect of a nonzero vapor velocity normal to the interface on the Maxwellian velocity distribution by inserting a coefficient (Γ). Additionally, two more coefficients, σ_c and σ_e, were added to account for the

fraction of molecules that strike the liquid-vapor interface and condense, or evaporate, respectively. Schrage's version of Eq. 5, therefore is:

$$J_m = \left(\frac{M}{2\pi R}\right)^{1/2} \left[\Gamma \sigma_c \frac{P_g}{T_g^{1/2}} - \sigma_e \frac{P_f}{T_f^{1/2}} \right]$$

(A.4)

Values for Γ are calculated using:

$$\Gamma = exp(-a^2) + a\pi^{1/2}\left[1 + erf(a)\right]$$

(A.5)

where the constant "a" represents the ratio of the overall speed of the vapor to a characteristic molecular velocity. The expression that relates the constant "a" to the molecular flux J_m is:
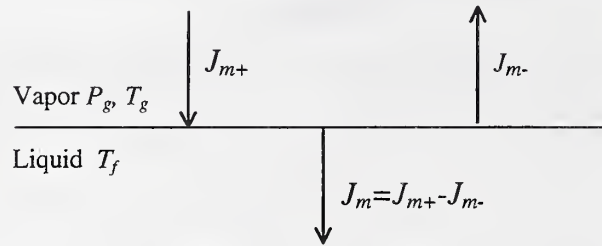
$$a = \frac{J_m}{P_g(2M/RT_g)^{1/2}}$$

(A.6)

Figure A.1 - Condensation process

Appendix B: Kraay And Rite Derivation

To derive an expression for J_m for use in Eq. 2, Kraay and Rite (1997) simplified Eq. A.4 from the kinetic theory of condensation by making several assumptions. Both σ_c and σ_e were assumed to be equal to one. This assumption is commonly made due to the difficulty of measuring the values of the condensation and evaporation coefficients. For example, Butterworth (1977) suggests that setting σ_c equal to 0.8 is a good engineering approximation for all circumstances.

To further simplify the expression for J_m, the temperature jump at the interface was taken to be equal to zero (i.e., $T_f = T_g$). With these assumptions, Eq. A.4 becomes:

$$J_{m,net} = \left(\left(\frac{M}{2\pi RT} \right)^{1/2} P_g \right) \cdot \frac{2\rho_g}{2\rho_g - \rho_{ig}} \left[1 - \frac{P_f}{P_g} \right] = J_m \frac{2\rho_g}{2\rho_g - \rho_{ig}} \left[1 - \frac{P_f}{P_g} \right] \tag{B.1}$$

where ρ_g is the actual vapor density, and ρ_{ig} is vapor density calculated by means of the ideal gas law.

Because the kinetic theory does not provide knowledge of the pressure at the liquid-vapor interface from the liquid and vapor sides (P_f and P_g respectively), Kraay and Rite (1997) assumed that P_f was equal to the saturation pressure evaluated at the wall temperature and P_g was equal to the saturated vapor free stream pressure.

Kraay and Rite's third assumption leads to a simplified expression which describes a condensation process where the ratio of the vapor mass to total mass (vapor quality) is constant. However, as previously stated, in-tube condensation is a strong function of the vapor quality. To remedy this inconsistency, Kraay and Rite (1997) assumed that the relation between the vapor quality and the net molecular flux was linear. At a vapor quality of 100 %, the net molecular flux is defined by Eq. A.4. Conversely, at a quality of zero, the net molecular flux is zero because there is no vapor to be condensed. The resulting equation that satisfies the above two quality-flux boundary conditions is:

$$J_{m,net} = J_m \frac{2\rho_g}{2\rho_g - \rho_{ig}} \left[1 - \frac{P_f}{P_g} \right] \cdot x \tag{B.2}$$

Equation B.2 represents the molecular flux of condensing vapor perpendicular to the liquid-vapor interface. The molecular flux carries with it the energy of the vapor state that will be released to the vapor upon its condensation to liquid. The heat flux due to the phase change component of the condensation process can be expressed as the product of $J_{m,net}$ and the latent heat of condensation:

$$\frac{dq_{lat}}{dA} = J_m \frac{2\rho_g}{2\rho_g - \rho_{ig}} \left[1 - \frac{P_f}{P_g} \right] \cdot x \cdot i_{fg} \qquad (B.3)$$

The sensible heat component represents the amount of subcooling experienced by the condensed liquid. The sensible heat flux can be expressed as the heat transfer coefficient times the temperature difference between the liquid at the wall and the liquid at the vapor-liquid interface. The expression of the total heat flux is then the sum of the phase change and sensible heat flux:

$$\frac{dq}{dA} = J_m \frac{2\rho_g}{2\rho_g - \rho_{ig}} \left[1 - \frac{P_f}{P_g} \right] \cdot x \cdot i_{fg} + \frac{h}{c_{pl}} \left(i_f - i_{fw} \right) \qquad (B.4)$$

Superposing a liquid subcooling heat flux to a latent heat flux allows the total heat flux to reduce to the only the sensible heat flux at the cessation of condensation.

Kraay and Rite further simplified Eq. B.4 by coupling the latent and single phase terms with the following assumption (for which they offer no justification):

$$J_m \frac{2\rho_g}{2\rho_g - \rho_{ig}} = \frac{h}{c_{pl}} \qquad (B.5)$$

Substituting Eq. B.5 into Eq. B.4 gives:

$$\frac{dq}{dA} = J_m \frac{2\rho_g}{2\rho_g - \rho_{ig}} \left[\left[1 - \frac{P_f}{P_g} \right] \cdot x \cdot i_{fg} + \left(i_f - i_{fw} \right) \right] \tag{B.6}$$

Using Eq. B.6 Kraay and Rite calculated J_m from the experimental data available in the literature.

Figures B.1 and B.2 compare the variation of the J_m and h_{ref} (traditional heat transfer coefficient) coefficients for condensing R32 normalized by the values at the test section entrance for parallel and counterflow, respectively. The data are taken from Kedzierski and Gonclaves (1999) and have an expanded uncertainty of approximately $\pm$ 5 % for 95% confidence. These data show a significant variation of the coefficient J_m with heat flux along the pipe. The scatter of J_m along the pipe is comparable to the variation of h_{ref}. It was believed that one benefit of the enthalpy-difference approach was that the J_m was constant with respect to quality. Figures B1 and B.2 illustrate that this is not strictly true. Figure B.3 also shows that there is considerable scatter in the variation of J_m versus the vapor quality for the Kedzierski and Gonclaves (1999) data.
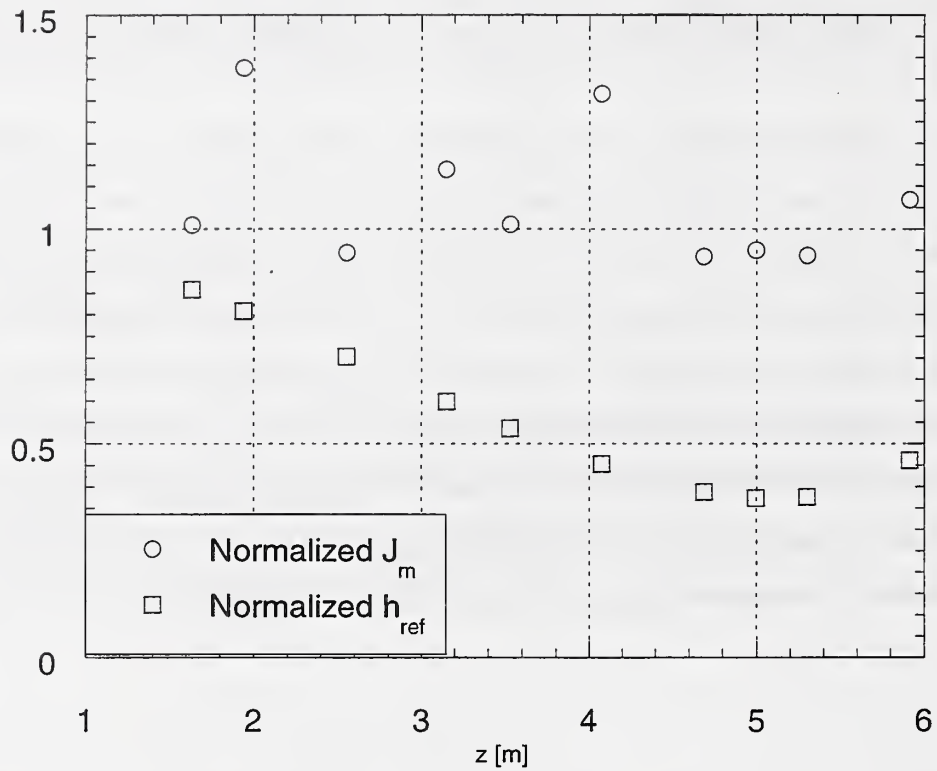
Figure B.1-Normalized Kraay and Rite J_m and Normalized h vs the distance along the pipe

Micro-fin tube, R32, condensation, $\alpha=18°$, $D_h=5.45$, Re=7715, Pr=0.278, Parallel flow configuration

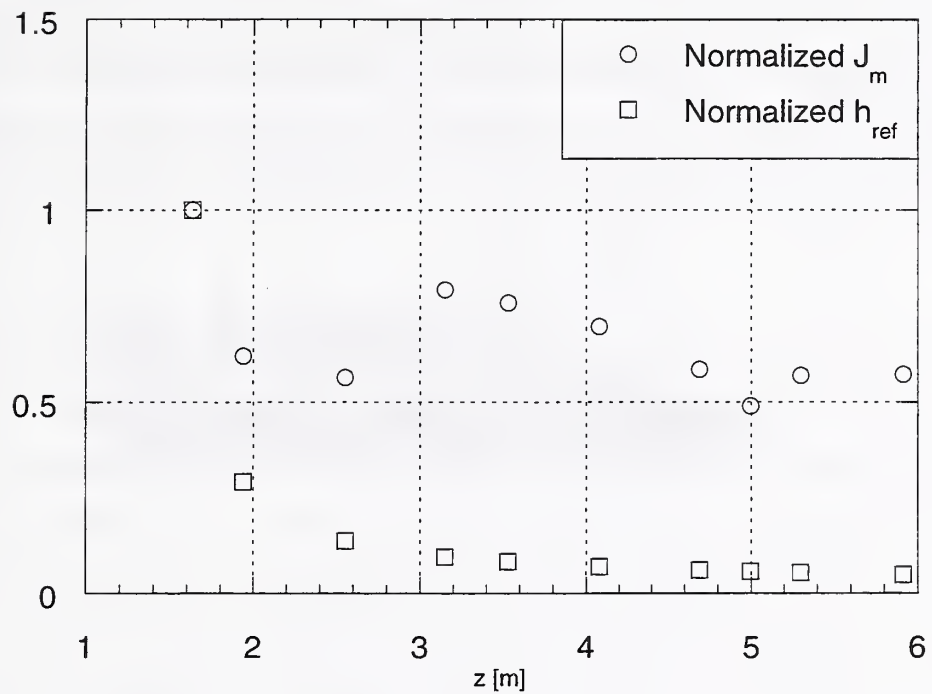Figure B.2-Normalized Kraay and Rite J_m and Normalized h vs the distance along the pipe Micro-fin tube, R32, condensation, $\alpha=18°$, $D_h=5.45$, Re=7715, Pr=0.278, counterflow configuration
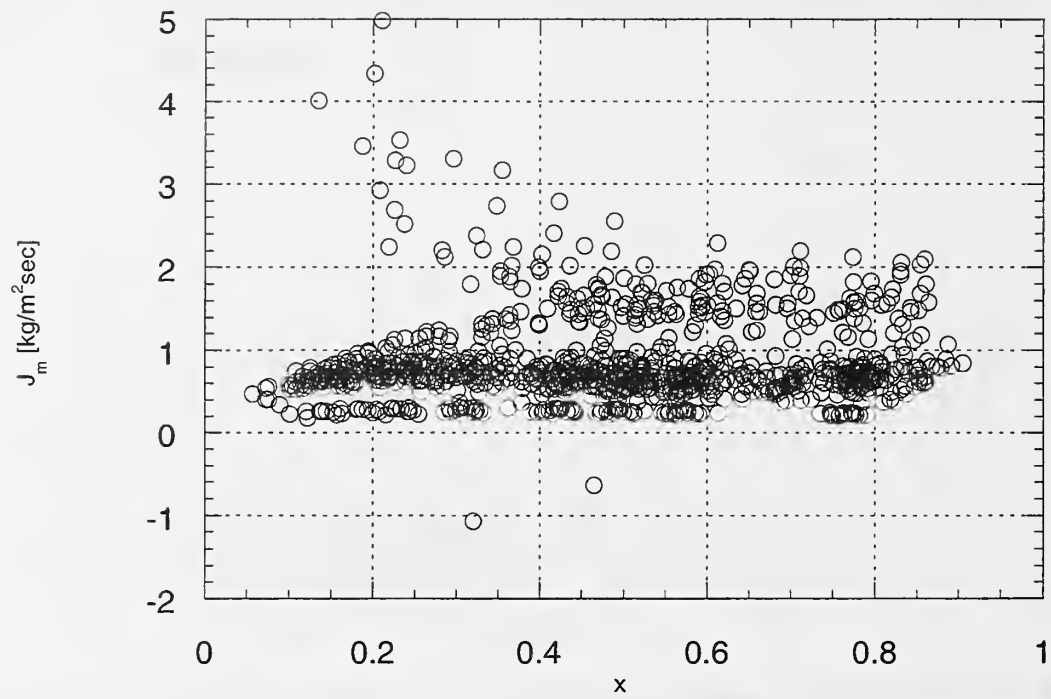
Figure B.3- Variation of Kraay and Rite's Jm with vapor quality

Appendix C: Discussion Of Kraay And Rite Assumptions

In Appendix B, the assumption made by Kraay and Rite are show. In this Appendix, the assumptions made in Kraay and Rite (1997) are discussed. The assumption used to derive Eq. B.6, where P_f is calculated as the saturation pressure of the liquid at wall temperature conditions is not consistent with the existence of subcooled liquid at the wall. This assumption contradicts the superposition principle used to obtain Eq. B.4, where the liquid at the wall is taken to be subcooled.

Also, an inconsistency arises in Eq. B.4 when the configuration of the heat transfer fluid is counterflow. For parallel flow, the total heat flux diminishes from the inlet to the outlet of the pipe due to a smaller temperature difference between the heat sink and condensing vapor. Equation B.4 correctly reflects this trend where the total heat flux (left term in Eq. B.4) diminishes with increasing distance along the pipe (z). The latent heat transfer (first term of the right side of Eq. B.4) decreases with z due to the linear dependence on x (in fact, x diminishes along to pipe), while the sensible part of the heat flux is negligible compared to the total heat flux. Conversely, for counterflow, the total heat flux increases with increasing z, while the latent heat diminishes with z. Consequently, because the latent heat flux typically represents over 90 % of the total, Eq. B.4 does not correctly predict the trend of heat flux with respect to pipe length.

The other observation seen in Eq. B.4 is that the total heat flux, as well as the sensible heat flux, passes through the inner area of the refrigerant pipe, while the latent heat flux passes through the liquid-vapor interface. Equation B.4 does not account for the difference in reference surface area for the latent and single phase heat fluxes. Consequently, this causes the energy balance not to be invalid.